Application of Hilbert Techniques to the Study of Subsynchronous Oscillations

Manuel Andrade, *Student member, IEEE,* and A. R. Messina, *Member, IEEE*

Abstract--This paper discusses the application of Hilbert transform based signal analysis techniques to the study of subsynchronous torsional oscillations in power systems with FACTS controllers. An analysis framework based on the Hilbert transform technique, for detection and quantification of nonlinear power system behavior is presented. The method is based on the Hilbert-Huang technique, which gives a time-energy-frequency representation of the data and enables the analysis of both the nonlinear and non-stationary responses of complex power systems to large perturbations.

The application of these procedures is illustrated on the IEEE second benchmark system for the analysis of subsynchronous resonance. The nonlinear spatio-temporal behavior of torque signals is examined for and it is concluded that power systems may exhibit a wealth of nonlinear dynamical characteristics including harmonic generation and nonlinear mode interaction.

Keywords: Power system transient stability, nonlinear systems, spectral analysis, subsynchronous resonance.

I. INTRODUCTION

THE analysis of transient behavior of power systems with Flexible ac Transmission System (FACTS) devices has been the subject of extensive study in recent years. FACTS devices offer a powerful alternative to increase the stability of the torsional modes of oscillation of a power system as well as to improve system operating flexibility [1], [2].

Of special interest are applications where FACTS devices may interact nonlinearly with the torsional modes of vibration of large turbine-generators [3]. With the current and future availability of an increasing number of nonlinear controllers, the onset of system oscillations is becoming more complex and unpredictable [4].

During the past few years there have been a number of theoretical studies undertaken for understanding the basic properties of the linear system response to small and large perturbations. Whilst it is possible to compute nonlinear behavior using several techniques, much of the attention in the past has been devoted to the understanding of nonlinear system performance using a variety of linear techniques [5]. The main shortcomings of these approaches are the requirements of linearity and stationarity or periodicity which render them invalid or uninformative for many applications.

Somewhat more general alternatives to conventional linear analysis are wavelet methods, the theory of evolutionary spectra, and Hilbert transform based signal analysis [6], [7]. A remarkably successful approach for studying the nonlinear behavior of time series is the Hilbert-Huang technique first derived by Huang *et al*. [8]. With this technique, complicated sets of nonlinear, non-stationary data sets can be decomposed into finite collections of intrinsic mode functions.

This paper extends our previous work on the application of the Hilbert transform [9] and concentrates on the analysis of nonlinear dynamic behavior in power systems with thyristor-controlled series capacitors. The application of these procedures is illustrated on the IEEE second benchmark system for the analysis of subsynchronous resonance (SSR). Hilbert spectral analysis is performed on out data files generated by nonlinear simulations using the EMTP, but the method is quite general and is applicable to any nonlinear, non-stationary signal.

II. PRELIMINARY CONCEPTS

A. The Hilbert Transform

In this section the use of the Hilbert transform for non-steady time series analysis is briefly considered. Let $u(t)$ be a real-valued signal. The Hilbert transform, $v(t)$, is [10]

$$v(t) = -\frac{1}{p} P \int_{-\infty}^{\infty} \frac{u(h)}{h-t}\, dh, \tag{1}$$

where P stands for the principal value of the integral in the Cauchy's sense. The inverse transform is given by

$$u(t) = \frac{1}{p} P \int_{-\infty}^{\infty} \frac{v(h)}{h-t}\, dh. \tag{2}$$

This pair of functions could be written in a convolution form as

$$v(t) = u(t) * \frac{1}{p\,t}, \tag{3}$$

$$u(t) = -v(t) * \frac{1}{p\,t}. \tag{4}$$

Taking the Fourier transform to the kernel of the Hilbert transform (HT), $\Theta(t) = 1/(p\,t)$, yields

$$\frac{1}{p\,t} \overset{F}{\Leftrightarrow} -\,\mathrm{jsgn}(w). \tag{5}$$

Applying the convolution to multiplication theorem of the Fourier transform results in

$$v(t) \overset{F}{\Leftrightarrow} V(w) = -\,\mathrm{jsgn}(w)U(w) \tag{6}$$

allowing the calculation of the Hilbert transform using the inverse Fourier transform of (6). Given $u(t)$ and $v(t)$, a complex analytic signal can be defined.

B. The Analytic Signal and the Hilbert Transform

Our implementation of the complex analytical signal follows

M. Andrade and A. R. Messina are with the Center for Research and Advanced Studies, National Polytechnic Institute, Guadalajara, 45232 Mexico (e-mail: mandrade@gdl.cinvestav.mx; aroman@gdl.cinvestav.mx

Presented at the International Conference on Power Systems Transients (IPST'05) in Montreal, Canada on June 19-23, 2005
Paper No. IPST05 - 172

that of Andrade *et al*. [9]. The analytic signal, $y(t)$, is a complex function of time defined as

$$y(t) = u(t) + v(t). \quad (7)$$

Making a coordinates change from rectangular to polar the following expressions are obtained:

$$u(t) = A(t)\cos[j(t)], \quad (8)$$

$$v(t) = A(t)\sin[j(t)]. \quad (9)$$

Hence, the analytic signal can be expressed as

$$y(t) = A(t)\,e^{jj(t)}, \quad (10)$$

where $A(t)$ and $j(t)$ are the instantaneous amplitude and instantaneous phase of the analytic signal, respectively, defined by

$$A(t) = \sqrt{u^2(t) + v^2(t)}, \quad (11)$$

$$j(t) = \arctan\frac{v(t)}{u(t)}. \quad (12)$$

In a similar manner, the instantaneous frequency can be expressed as

$$w(t) = \dot{j}(t) = \frac{u(t)\dot{v}(t) - v(t)\dot{u}(t)}{u^2(t) + v^2(t)}. \quad (13)$$

Hilbert analysis provides a method for determining the instantaneous power and frequency of a monocomponent signal. An extension of the notion of the analytic signal to multi-component signals is possible using the empirical mode decomposition (EMD) method introduced by Huang *et al*. [8].

C. The Empirical Mode Decomposition (EMD) Method

Hilbert analysis is based on a non-causal singular transformation termed empirical mode decomposition (EMD). In the Hilbert-Huang technique approach (HHT), The procedure to extract the intrinsic mode functions (IMF) from the signal is known as the sifting process and can be summarized as follows: (1) starting with the original signal, $x(t)$, set $h_1(t) = x(t)$, extract the local minima and local maxima from $h_i(t)$, (2) interpolate the local minima and local maxima with a cubic spline to form upper and lower envelopes respectively, and (3) obtain the mean of the upper and lower envelopes, $m_i(t)$, and subtract it form $h_i(t)$ to determine a new function $h_{i+1}(t) = h_i(t) - m_i(t)$. The above procedure is repeated until $h_{i+1}(t)$ satisfies the criteria of an IMF and then $c_j(t) = h_{i+1}(t)$.

Once the IMF components have been determined, the original signal can be reconstructed using the HT as

$$x(t) = \sum_{j=1}^{n} c_j(t) + r(t). \quad (14)$$

In the follows that the signal $x(t)$ can be re-expressed in terms of the Hilbert transform, as

$$x(t) \approx \mathrm{Re}\left\{\sum_{j=1}^{n} A_j(t)\exp\left(\mathrm{j}\int w_j(t)\,dt\right)\right\}. \quad (15)$$

Eq. (15) allows the instantaneous amplitude and instantaneous frequency to be represented as time functions.

D. The Hilbert Spectrum

The time-frequency distribution of the amplitude is known as the Hilbert amplitude spectrum, $H(w,t)$. The total amplitude contribution for each frequency value measure is given by the marginal spectrum

$$h(w) = \int_0^T H(w,t)\,dt. \quad (16)$$

Moreover, the energy fluctuation on the signal is provided by the instantaneous energy density level, IE, defined as [10]

$$\mathrm{IE}(t) = \int_w H^2(w,t)\,dw. \quad (17)$$

For a more detailed explanation of the Hilbert spectra in the context of this model, see [11].

III. Application

The system under study is the IEEE SBM for computer simulation of subsynchronous resonance [12]. Fig. 1 shows a one-line diagram of the system illustrating the location of a Thyristor-controlled Series Capacitor (TCSC) This system represents a 600 MVA, 2 pole, 22 kV turbo-generator supplying power through two parallel 500 kV transmission lines, one of which is series compensated, to an infinite bus.

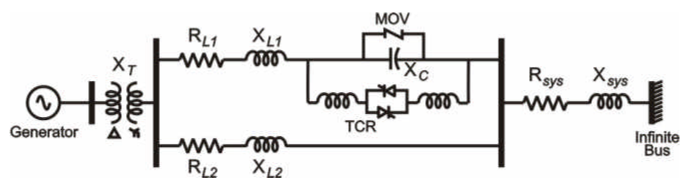

Fig. 1. The IEEE Second Benchmark Model for SSR studies.

Operating scenarios for SSR analysis included 1) system operation with conventional fixed compensation (no TCSC), and 2) the TCSC operating in enhanced constant power control mode [1], and 55% compensation. The parameters of the SBM are taken from [12].

A. Torsional System Model

The shaft mechanical model of the SBM comprises four rotating masses: a high-pressure (HP) turbine, a low-pressure (LP) turbine, a synchronous generator (GEN), and a rotating exciter (EXC). Fig. 2 shows the mechanical system for the SBM. The SBM exhibits two torsional modes at frequencies 23.63, and 31.97 Hz.

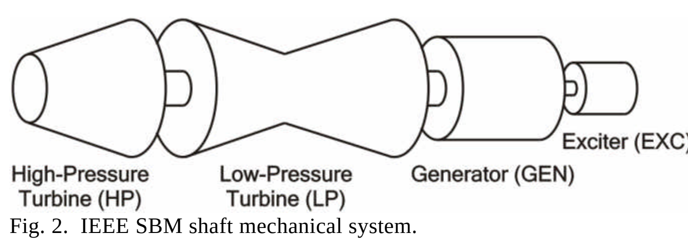

Fig. 2. IEEE SBM shaft mechanical system.

Table I gives the frequency and damping of torsional mode eigenvalues at 55% compensation. We next examine the onset of nonlinear behavior using both Fourier–based spectral analysis methods and Hilbert techniques.

TABLE I
Torsional Eigenvalues For 55% of Series Compensation

Mode	Eigenvalue	Frequency (Hz)	Damping
1	$-15.94824 \pm j\,148.45389$	23.62717	0.10681
2	$-17.28974 \pm j\,200.87426$	31.97013	0.08575

B. Nonlinear Time-Domain Simulation Studies

Detailed transient simulations have been performed in an attempt to develop an understanding of nonlinear dynamics. The study focuses on the torque amplification phenomena due to subsynchronous resonance.

The fault is a three-phase short-circuit through a fault reactance of 0.1 mH applied at $t = 0.17$ s on the high-voltage side of the generator step-up transformer, cleared after one cycle; this fault excites the torsional modes of the system and results in a complex dynamic behavior involving nonlinear subsynchronous oscillations. For reference, the peak values of the torques are given in Table II.

TABLE II
COMPARISON BETWEEN THE CALCULATED TORQUES AND THE SBM CASE A TORQUES

Torques	Simulation (pu)	SBM Case A (pu)	Error (%)
HP-LP	2.0118	1.97	2.1218
LP-GEN	4.1520	4.02	3.2836

Fig. 3 shows the transient torques resulting from this disturbance whilst the corresponding power spectrum of the shaft torques is presented in Fig. 4.

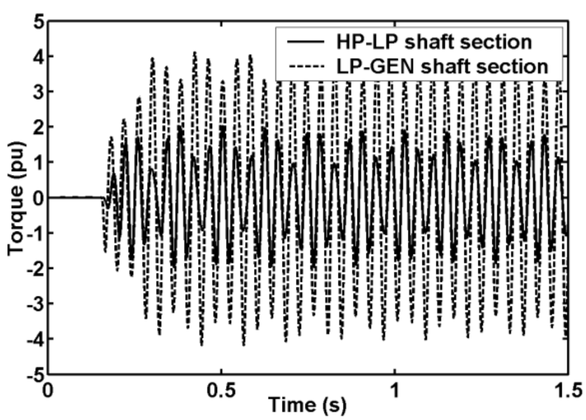

Fig. 3. Shaft torsional responses resulting from system perturbation.

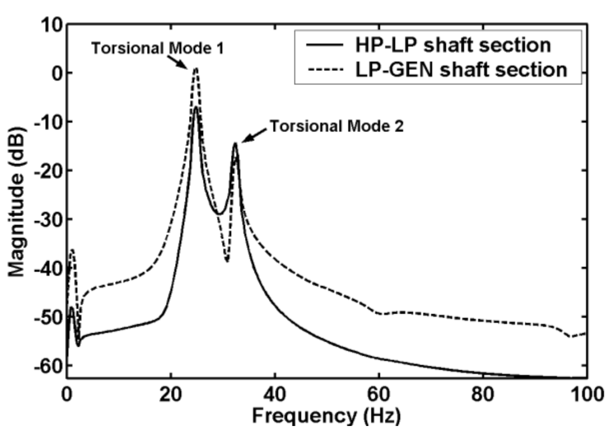

Fig. 4. Fourier power spectrum of shaft torque signals.

As expected from eigenanalysis, examination of the power spectra in Fig. 4 indicates the excitation of two modes at about 23.6 Hz and 32 Hz disclosing the presence of torsional modes 1 and 2.

C. Hilbert Spectrum and Instantaneous Frequency

To analyze the instantaneous attributes of the signals, the simulated data was first decomposed into a summation of modal components using the EMD technique. Fig. 5 shows the first four IMF for each of the torques depicted in Fig. 3.

For the HP-LP torque record, application of the EMD method yields, primarily, one dominant IMF. This essentially indicates that the original function can be approximated by a single modal function of varying amplitude and frequency; the effect is more pronounced for the LP-GEN torque in Fig. 5b.

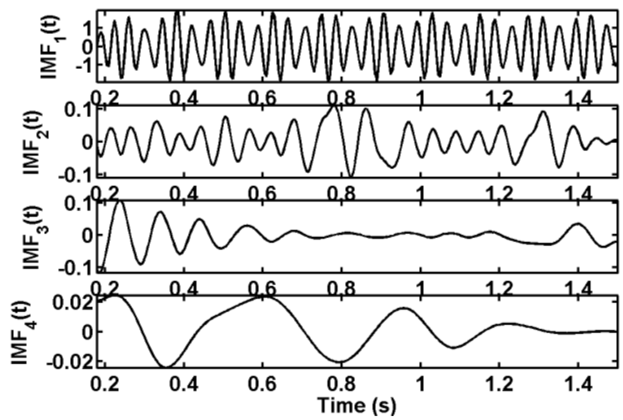

(a)

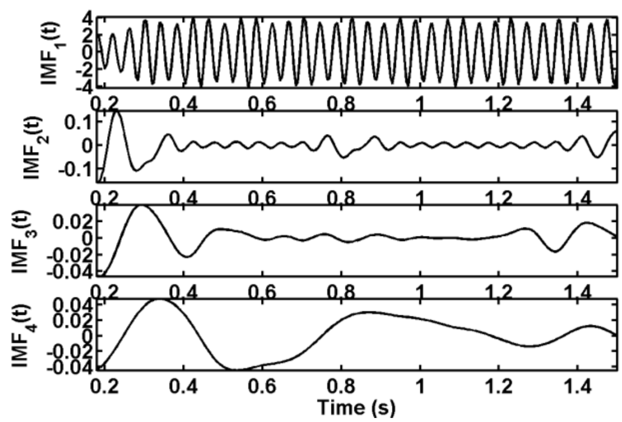

(b)

Fig. 5. The resulting intrinsic mode functions for the shaft torque signals; a) HP-LP shaft section, and b) LP-GEN shaft section.

Further insight into the nature of temporal behavior is obtained from the analysis of the instantaneous attributes of each IMF.

Fig. 6 shows the Hilbert spectrum of the torque signals. The nonlinear fluctuations observed in the plot reveal the presence of modulation between spectral components and indicate nonstationarity. Here, an IMF is associated with a local time scale of the data and can be amplitude and/or frequency modulated and even non-stationary. The first IMF is composed of the smallest time scale that corresponds to the highest frequency or fastest variation of the data; the frequency decreases as the index i of IMF_i increases.

For the HP-LP torque, examination of the Hilbert marginal spectrum for IMF in Fig. 6a shows a temporal behavior in which the frequency of the IMF oscillates about 28Hz (the average frequency of torsional modes 1 and 2) and 21 Hz, respectively, with varying amplitude and frequency, suggesting nonlinear interaction between these modes. Moreover, the Hilbert marginal spectrum shows the presence of a third IMF at about 10 Hz, of essentially constant frequency probably indicating sub harmonic modulation of IMF2. Analysis of the Hilbert spectrum of the IMF for the LP-GEN torque record in Fig. 5b leads to similar conclusions.

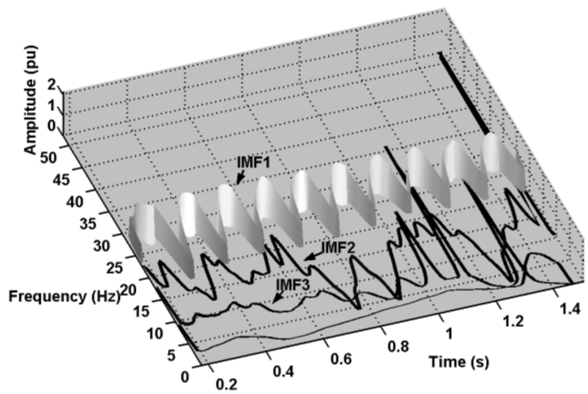

(a)

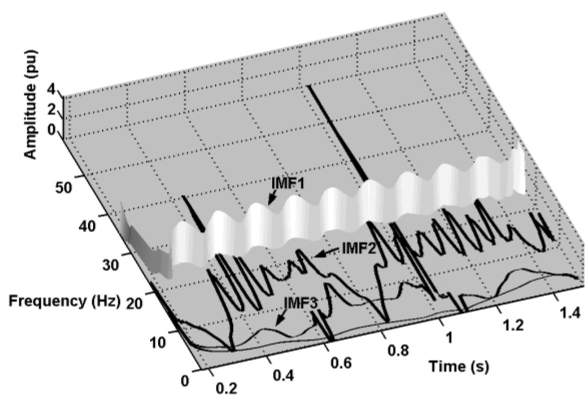

(b)

Fig. 6. Hilbert spectrum of the IMF associated with the shaft torque signals; a) HP-LP shaft section, and b) LP-GEN shaft section.

Also of interest, comparison of Fig. 5a and Fig. 5b reveals that non-stationarity is more pronounced in the HP-LP record. Thus, for instance, the instantaneous frequency of the IMF 1 and 2 for the HP-LP record exhibit larger variations than the corresponding frequencies for the LP-GEN record.

D. Damping of Torsional Oscillations by Means of TCSC

The general structure of the TCSC used in the studies is shown in Fig. 7. To examine the impact of the TCSC on torsional damping an enhanced constant-power control mode [13] is adopted. In this arrangement, the main control loop is a fast current control loop. The controller has a secondary loop responsible for power control: the power controller generates the current order of the inner (current) controller. This arrangement provides flexibility and can be made to respond extremely fast to large system disturbances, whilst at the same time provide the necessary slower response for electromechanical modes of oscillation.

Figure 8 shows the transient torques and the total (line) TCSC current. For completeness, the line current with conventional fixed compensation is also shown.

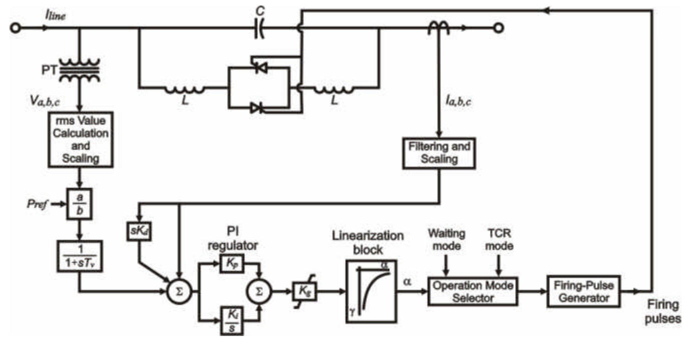

Fig. 7. Block diagram of the enhanced TCSC control structure.

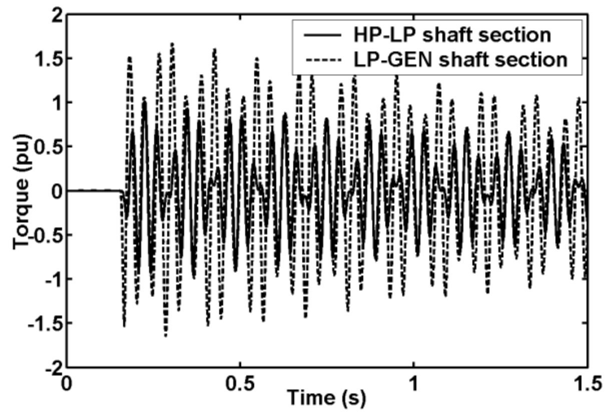

(a)

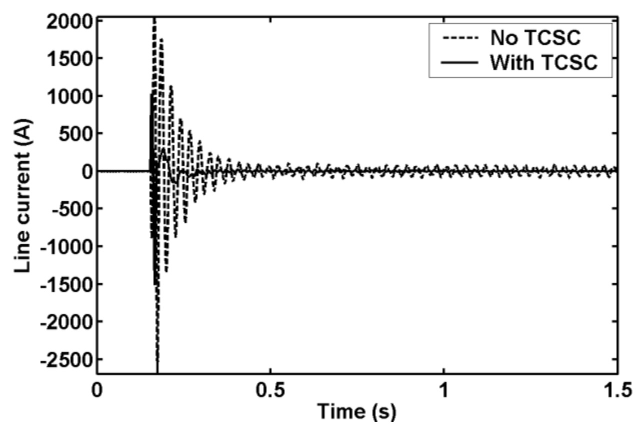

(b)

Fig. 8. a) Shaft torques, and b) Total TCSC current following a system contingency.

Examination of the time domain results in Fig. 8 shows that the use of a TCSC improves SSR behavior and leads to a more damped system response. This is manifested by decreased peak torques (refer to Table III) and more damped oscillations. Other simulations reveal that the use of TCSC leads to enhanced voltage regulation and can provide additional damping to electromechanical power system oscillations.

In order to further investigate nonlinear effects in the shaft torques, Fourier-based spectral analysis methods were applied to the shaft torque signals. Fig. 9 compares the power spectra of the HP-LP torque and the LP-GEN torque for the case with fixed compensation and with TCSC. Simulation results indicate that the TCSC has a strong impact on the damping of both torsional modes 1 and 2 and may increase nonlinear behavior.

TABLE III

TORQUE AMPLIFICATION COMPARISON

Compensation Scheme	HP-LP Peak Torque (pu)	LP-GEN Peak Torque (pu)	Torque Amplification (%)
Fixed compensation	2.0118	4.1520	106.3823
Thyristor controlled compensation	0.9789	1.6583	69.4044

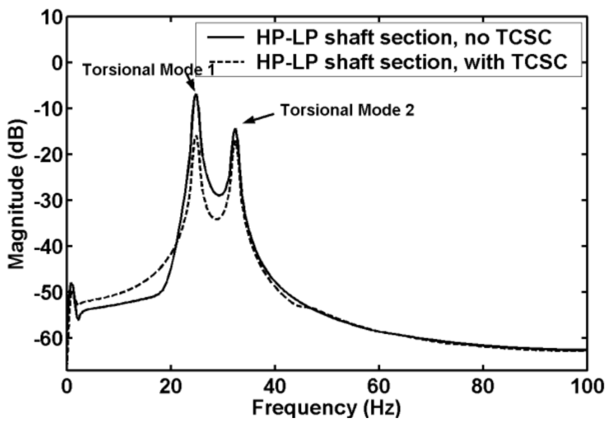

(a)

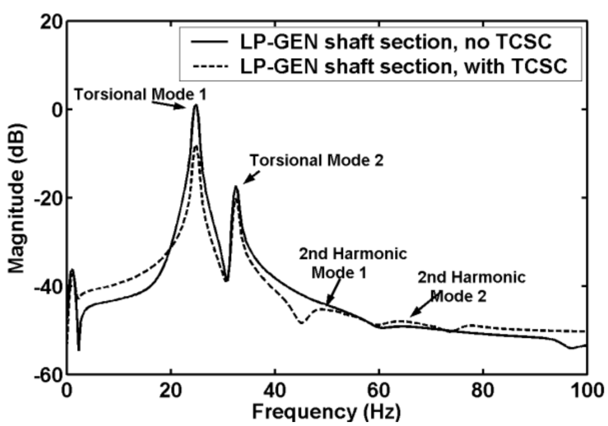

(b)

Fig. 9. Fourier spectra of the a) HP-LP shaft section, and b) LP-GEN shaft section, torque signals.

Of particular significance: the analysis of the Fourier spectra in Fig. 9b shows that the use of TCSC increases nonlinearity. Manifestations of this effect are seen in the relatively large components of the torsional mode harmonics at 0.50 Hz and 0.64Hz. Application of the EMD-Huang method to the HP-LP torque record yields seven IMF; the first four of them are shown in Fig. 10a. Comparison of Figs. 10a and 5a shows that the magnitude of IMF2 through to IMF4 relative to IMF1 increases, thus indicating an increase in nonlinear effects for both the HP-LP torque and the LP-GEN-torque. Further, the analysis shows clearly that more intrinsic mode functions are required to capture the true system dynamics.

A deeper insight into the nature of this behavior is obtained from the Hilbert spectrum in Fig. 11. Careful analysis of the spectra indicates that the inclusion of dynamic series compensation modifies nonlinear behavior and the time-varying characteristics of the underlying nonlinear dynamical system.

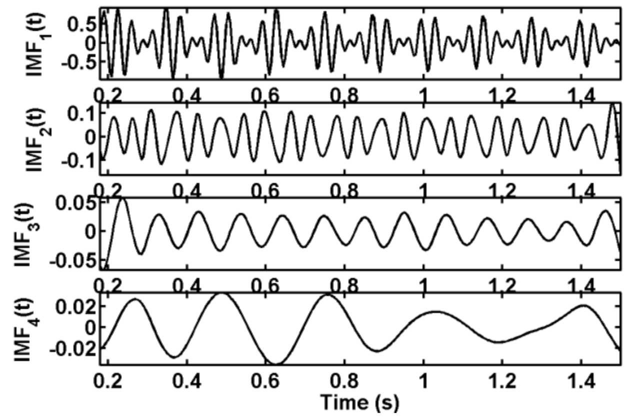

(a)

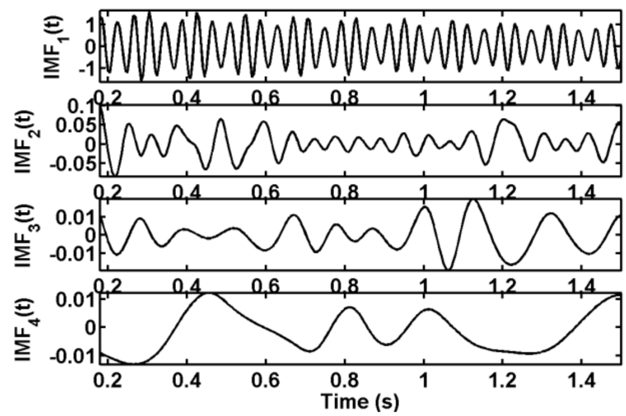

(b)

Fig. 10. Intrinsic mode functions resulting after apply the EMD on a) the HP-LP torque signal, and b) the LP-GEN torque signal.

Finally, the analysis of the Fourier spectra of each IMF associated with the LP-GEN record in Fig. 12 indicates that the incorporation of a TCSC results in harmonic generation. The other peaks in the Fourier spectra in Fig. 12b may indicate nonlinear interaction between primary spectral components but this is not investigated in this research. It should be noted that Fourier analysis of the original data fails to see the lower frequency components. Additional studies are needed to be conducted to determine nonlinear behavior arising from nonlinear modal interaction between control modes and electromechanical modes as well as to determine the underlying nature of these components.

IV. CONCLUSIONS

Nonlinear characterization of time series data presents challenging and difficult problems. Hilbert spectral analysis is able to capture the rich dynamics of a complex nonlinear spatio-temporal system and offers a much sharper frequency analysis. The method is adaptive and requires no prior knowledge of system characteristics.

Results from these studies indicate that nonlinear oscillations may involve interaction between the fundamental frequencies. These interactions result in significant modulation of the primary frequencies and lead to nonlinear and non-stationary behavior. There is also evidence of nonlinear interactions between the primary frequency components but this is to be further investigated. Further studies are needed to assess the nature of the underlying nonlinear behavior.

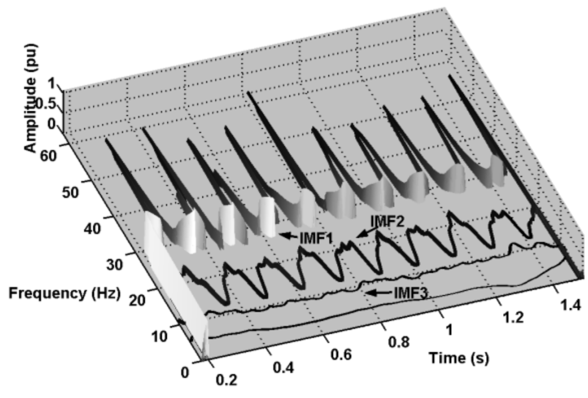

(a)

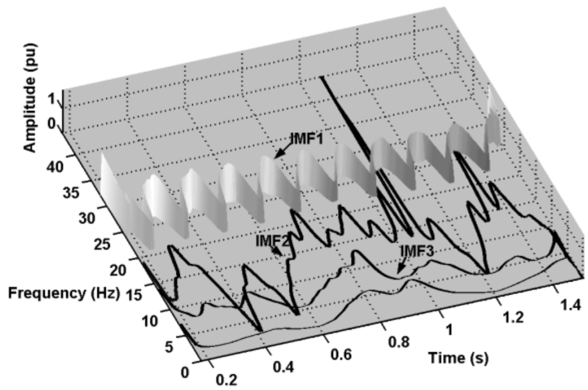

(b)

Fig. 11. Hilbert spectra of a) the HP-LP shaft section, and b) LP-GEN shaft section signals, with TCSC compensation.

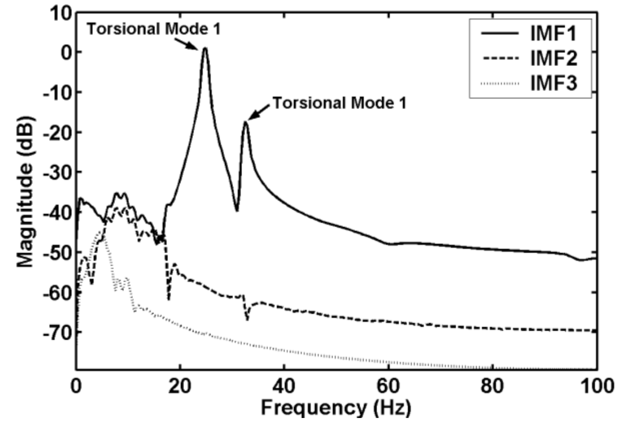

(a)

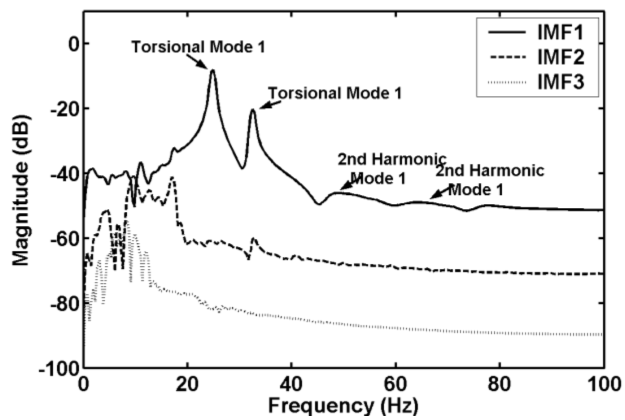

(b)

Fig. 12. Fourier spectra of LP-GEN shaft section torque signal IMF: a) with no TCSC, and b) with TCSC.

V. REFERENCES

[1] Luiz A. S. Pilotto, Andre Bianco, Willis F. Long, and Abdel-Aty Edris, "Impact of TCSC control methodologies on subsynchronous oscillations," *IEEE Trans. Power Syst.*, vol. 18, pp. 243-252, Jan. 2003.

[2] N. Rostamkolai, R. J. Piwko, E. V. Larsen, D. A. Fisher, M. A. Mobarak, A. E. Poitras, "Subsynchronous torsional interactions with static VAR compensators – Influence of HVDC," *IEEE Trans. Power Syst.*, vol. 6, pp. 255-261, Feb. 1991.

[3] J. J. Paserba, E. V. Larsen, C. E. Grund, and A. Murdoch, "Mitigation of inter-area oscillations by control," in *Proc. 1994 IEEE Symposium on Inter-Area Oscillations in Power Systems*, pp. 103-117.

[4] A. R. Messina, V. Vittal, "Assessment of nonlinear modal interaction using higher-order statistics," *IEEE Trans. Power Syst.*, to be published.

[5] Task Force 07 of Advisory Group 01 of Study Committee 38, "Analysis and control of power systems oscillations," CIGRE, Paris, Final Report, Dec. 1996.

[6] Steven R. Long, et. al., "The Hilbert techniques: An alternate approach for non-steady time series analysis," *IEEE-GRS-S Newsletter*, pp. 6-11, 1992.

[7] M. B. Priestley, "Multivariable series prediction" in *Spectral Analysis and Time Series*, vol. 2, London: Academic Press, 1981.

Norden E. Huang, Z. Shen, and S. R. Long, M. C. Wu, E. H. Shih, Q. Zheng, C. C. Tung, and H. H. Liu, "The Empirical mode decomposition and the Hilbert spectrum for nonlinear and non-stationary time series analysis," *Proc. of the Royal Society of London, A*, vol. 454, pp. 903-995, 1998.

[8] M. A Andrade, A. R. Messina, C. A. Rivera, and D. Olguin, "Identification of instantaneous attributes of torsional shaft signals using the Hilbert transform," *IEEE Trans. Power Syst.*, vol. 19, pp. 1422-1429, Aug. 2004.

[9] D. Gabor, "Theory of communication," *Proc. IEE*, vol. 93, pp. 429-457, 1946.

[10] Albena D. Veltcheva, "Wave and group transformation by a Hilbert spectrum," *Coastal Engineering Journal*, vol. 44, pp. 283-300, 2002.

[11] IEEE Subsynchronous Resonance Working Group of the Power System Engineering Committee, "Second benchmark model for computer simulation of subsynchronous resonance," *IEEE Trans. Power Apparatus and Systems*, vol. 104, pp. 1057-1066, May. 1985.

VI. BIOGRAPHIES

Manuel Andrade (S'98) was born in Michoacan, Mexico in 1979. He received the B.Sc. degree in electrical engineering from the Saltillo Institute of Technology, Saltillo, Mexico, in 2000, and the M. Sc. degree in 2002 from the Center for Research and Advanced Studies (CINVESTAV), National Polytechnic Institute (IPN), Guadalajara, Mexico, where he is currently pursuing the Ph.D. degree.

A. R. Messina received the M. Sc. degree (Honours) in Electrical Engineering–Power Systems from the National Polytechnic Institute of Mexico (IPN) in 1987 and the Ph.D. degree in Electrical engineering from Imperial College of Science Technology and Medicine, U.K in 1991. He is currently a Professor at CINVESTAV Mexico.